Decelerating and bunching molecules with pulsed traveling optical lattices

Guangjiong Dong, Weiping Lu, and P. F. Barker

Department of Physics, School of Engineering Physical Sciences, Heriot-Watt University, Edinburgh EH14 4AS, United Kingdom

(Received 9 May 2003; published 23 January 2004)

We investigate the deceleration and bunching of cold molecules in a pulsed supersonic jet using a far-off-resonant optical lattice traveling with a constant velocity. Using an analytical treatment, we show that by choosing the lattice velocity equal to half the supersonic beam velocity and by optimizing the pulse duration, a significant fraction ($\sim 33\%$) of translationally cold (1 K) CO molecules from a supersonic molecular beam can be decelerated to zero velocity, and simultaneously bunched in velocity space. Due to the large difference of polarizability to mass ratio between the buffer gas and the CO molecules in the pulsed jet, the buffer gas can be precluded from the fraction of stationary molecules by choosing a suitable pulse duration. Furthermore, we find that spatial bunching within the optical lattice is induced and the position of the bunch within the lattice can be chosen by varying the lattice velocity.

I. INTRODUCTION

In recent years, there has been strong interest in extending the well-established techniques developed for cooling and trapping of atoms to molecules [1]. The creation of cold stationary molecules offers the capability of ultrahigh-resolution molecular-beam spectroscopy [2], ultracold chemistry [3,4] and collisions [5–8] as well as the possibility of a molecular Bose-Einstein condensation [9,10]. However, the well-developed laser cooling methods for atomic species are not applicable to the cooling of molecules because of the complex molecular energy structure leading to a lack of closed cycling transitions [11].

Over the last few years, four approaches have been demonstrated for creating cold molecules. The *first* is to use photoassociation of ultracold alkali-metal atoms [12]. The formation of ultracold molecules arises from the deexcitation of excited molecules created by photoassociating colliding atoms into the molecules [13–19]. The created molecules are translationally cold (typically, <1 mK). However, they are not vibrationally cold as they are distributed over a larger number of vibrational states. Recently two-step photoassociation [20] and stimulated Raman photoassociation [21] have been performed to generate state-selected molecules. A second technique uses buffer-gas cooling combined with magnetic trapping [22]. Here paramagnetic molecules such as CaH are cooled down to temperatures in the 100 mK range by collision with a cryogenic helium gas, while confined in a magnetic trap. Essential to the success of the technique is that the spin-relaxation cross section must be much smaller than the elastic collision cross section [22]. A third technique is to use a supersonic expansion to produce a high density ($\sim 10^{12}$ cm^{-3}) of translationally cold molecules (~ 1 K) [23] coupled with time-varying electric fields to slow the beam [24–29]. In this scheme any polar molecule entering an electric field gains Stark energy while losing its kinetic energy. After the electric field is switched off, molecules do not gain the lost kinetic energy, and are therefore decelerated. In these experiments, an array of electric-field stages are switched on and off alternatively to create a traveling potential well. The switching time is gradually increased to lower the velocity of the traveling potential well. In this way, deceleration of an ensemble of molecules, such as NH$_3$ and CO, was demonstrated in recent experiments [24–29]. A fourth technique uses a supersonic nozzle mounted at a tip of a high-speed rotor, where the flow velocity of gas emerging from the nozzle was canceled by the rotor velocity in the opposite direction [30,31]. The velocities of molecular beams of Xe or O$_2$ seeded in Xe have been slowed to a few tens of meters per second with this technique. Other approaches have been proposed for decelerating molecules in a molecular beam. Friedrich studied slowing of supersonically cooled atoms and molecules by time-varying nonresonant induced dipole forces [32]. In this approach, the molecules are scooped at right angles by a nonresonant laser beam steered by a scanner and decelerated on a circular path by gradually reducing the beam's angular speed. More recently, analogous to the Stark decelerator, Barker *et al.* have proposed a microlinear decelerator (decelerating optical lattice) that could be used to decelerate a fraction of any molecular beam to zero velocity [33]. The microlinear decelerator is created by two counterpropagating far-off-resonant optical fields, one of which has a linear frequency chirp. Furthermore, molecules can be trapped and transported by the optical lattice when the direction of the acceleration of the optical lattice is opposite to that of beam velocity. In this scheme, polar and even heavy nonpolar molecules such as I$_2$ can be slowed to be nearly stationary by the optical lattice with intensities in the range of 10^{10} W cm^{-2} [33].

Recently, bunching for storage of cold molecules and other applications has been pursued with time-varying electric fields [34]. Velocity bunching is a dynamic localization of molecules within the lattice at a particular velocity with a delocalization in phase space required to maintain phase-space density. This process has been demonstrated to create an ensemble of molecules with a longitudinal temperature width of 250 μK [34], which could be used to increase the phase contrast in molecular-beam diffraction studies. Spatial bunching, which is a localization of molecules at a particular phase, has been demonstrated to be highly desirable for trapping and storing cold molecules. For example, it can be utilized to optimize the number of molecules loaded from the
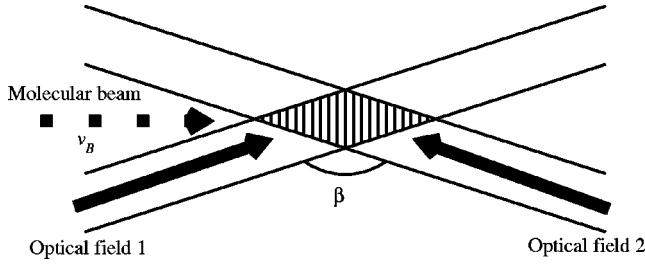
FIG. 1. A moving optical lattice is created by two optical fields with different frequencies intersecting at an angle of $\beta \approx 180°$. A molecular beam with longitudinal velocity v_B is injected into the interference pattern of the two crossed optical fields.

decelerated beam into an electrostatic quadrupole trap [26]. The spatial bunching could also be advantageous for collision studies [34] and lithography [35,36].

In this paper, we study an approach that applies a traveling far-off-resonant optical lattice, with constant velocity, to slow a fraction of cold molecules in a pulsed supersonic jet to nearly zero velocity. Further, we show that this scheme is capable of bunching molecules in position space or velocity space. In Sec. II, we study the dynamics of the molecules in the optical lattice for analyzing the capability of the optical lattice to decelerate and bunch molecules in the pulsed molecular jet. In addition, we determine the optimal optical lattice velocity for creating the maximum fraction of stationary molecules. We present an analytical formula for the velocity and position distribution of molecules in the optical lattice in Sec. III, and in Sec. IV we apply our analysis to a cold (1 K) supersonic beam of CO molecules and show that a significant fraction ($\sim 33\%$) of molecules can be decelerated and simultaneously bunched in velocity space. Finally, we demonstrate that spatial bunching can be achieved and the bunching position can be controlled by the optical lattice velocity in Sec. V.

II. PRINCIPLES FOR DECELERATING AND BUNCHING OF MOLECULES WITH A TRAVELING OPTICAL LATTICE

We consider molecules in a molecular beam with a velocity v_B, interacting with a traveling optical lattice, as shown in Fig. 1. The traveling optical lattice is formed by two nearly counterpropagating optical pulses, $\varepsilon_1(\mathbf{r},t) = E_1(t)\sin(\mathbf{k}_1 \cdot \mathbf{r} - \omega_1 t)$ and $\varepsilon_2(\mathbf{r},t) = E_2(t)\sin(\mathbf{k}_2 \cdot \mathbf{r} - \omega_2 t)$, where E_1 and E_2 are the amplitudes of the two optical fields, and $\mathbf{k}_1$ and $\mathbf{k}_2$ are the wave vectors of each field. The frequencies ω_1 and ω_2 are chosen to be far-off-resonant from the lowest single photon transition to form a quasielectrostatic potential [37,38]. The temporal profile of each field has a top hat, so that $E_1(t) = E_2(t) = E_0$ for $t < t_d$ where t_d is the pulse duration, otherwise $E_1(t) = E_2(t) = 0$ [39–42].

At the intersection of the two nonresonant fields, molecules gain the dipole potential,

$$U(\mathbf{r},t) = -\alpha E_1 E_2/2 \cos[(\mathbf{k}_1 - \mathbf{k}_2) \cdot \mathbf{r} - (\omega_2 - \omega_1)t], \quad (1)$$

where α is the polarizability. The dipole forces in the longitudinal and transverse directions are respectively given by

$$F_\parallel = -F_0 \sin[(\mathbf{k}_1 - \mathbf{k}_2) \cdot \mathbf{r} - (\omega_2 - \omega_1)t], \quad (2)$$

$$\mathbf{F}_\perp = F_\parallel (\mathbf{k}_{1\perp} - \mathbf{k}_{2\perp})/q, \quad (3)$$

where $F_0 = \alpha q E_1 E_2/2$ is the maximum force, and where $q = |\mathbf{k}_{1\parallel} + \mathbf{k}_{2\parallel}|$. The vectors $\mathbf{k}_{1\parallel}$ and $\mathbf{k}_{2\parallel}$ ($\mathbf{k}_{1\perp}$ and $\mathbf{k}_{2\perp}$) are the longitudinal (transverse) components of the vectors $\mathbf{k}_1$ and $\mathbf{k}_2$. In the nearly counterpropagating configuration shown in Fig. 1, the included angle between the optical fields and the molecular beam is less than 2.5°. Therefore, the magnitude of the transverse wave vectors $\mathbf{k}_{1\perp}$ and $\mathbf{k}_{2\perp}$ are small compared to the longitudinal components. Since there is small difference in the frequencies of the two beams, $\mathbf{k}_{1\perp} \approx \mathbf{k}_{2\perp}$, and the ratio $|(\mathbf{k}_{1\perp} - \mathbf{k}_{2\perp})/q|$ is much less than 1% for nearly counterpropagating beams ($\beta \gtrsim 175°$ in Fig. 1) the magnitude of the dipole force $F_\perp$ in the transverse direction is much less than the longitudinal force $F_\parallel$. To show that we can neglect the transverse force in further calculations we estimate its effect on the molecular beam for the duration of the optical field t_d. The transverse velocity change induced by the force is given by $|\Delta v_\perp| < |F_0(\mathbf{k}_{1\perp} - \mathbf{k}_{2\perp})/(mq)|t_d$, and the transverse displacement is $|\Delta s_\perp| < |v_{\perp 0} t_d| + |F_0(\mathbf{k}_{1\perp} - \mathbf{k}_{2\perp})/(qm)|t_d^2/2$, where m is the mass of the molecule and $v_{\perp 0}$ is the initial transverse velocity. For a CO (mass $m = 4.65 \times 10^{-26}$ kg, $\alpha = 2.15 \times 10^{-40}$ C m²/V) molecular beam at temperature of 1 K (the most probable velocity of $v_m \approx 25$ m/s), we estimate a transverse velocity change of $|\Delta v_\perp| < 6.19$ μm/s, and a transverse displacement of $|\Delta s| < 50$ nm. These calculations are carried out using optical fields with an intensity 8.29×10^{11} W/cm², $q = 1.57 \times 10^7$/m, a pulse duration of $t_d = 10$ ns, and the ratio $|(\mathbf{k}_{1\perp} - \mathbf{k}_{2\perp})/q| = 1\%$. The initial transverse velocity $v_{\perp 0}$ we used in this estimation is twice the most probable velocity determined by the temperature. As in this example, where the duration of typical experimental schemes is in the nanosecond range, the transverse velocity change $|\Delta v_\perp|$ induced by the potential is much less than the most probable velocity v_m, and the transverse displacement $|\Delta s|$ is much less than the typical width of the optical lattice (100 μm). Therefore, the weak transverse force $F_\perp$ does not significantly change the transverse position or velocity of molecules within the pulse duration we consider. We conclude that only a very small fraction of the molecules will enter or escape from the potential during these time periods, and therefore, the optical interference pattern produced by two intersecting optical fields as shown in Fig. 1 is essentially a quasi-one-dimensional optical lattice. Thus, the dipole force exerted on molecules in the nearly counterpropagating optical fields is effectively given by the longitudinal force $F_\parallel$ and now $(\mathbf{k}_{1\perp} - \mathbf{k}_{2\perp}) \cdot \mathbf{r}_\perp$ in Eq. (2) can be neglected, and $F_\parallel$ is given by

$$F_\parallel = -F_0 \sin[q(x - v_L t)], \quad (4)$$

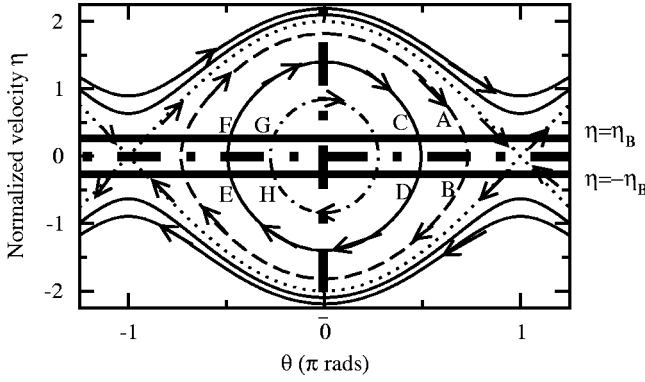where $v_L = (\omega_2 - \omega_1)/q$, and the equation of motion for molecules is given by

FIG. 2. Trajectories in the phase space (θ, η) are calculated by Eqs. (6) and (8). Each line is an equal-energy line and the arrows show the direction of the motion in the lattice frame. The dotted lines are separatrix and the region enclosed by the separatrix is a trapping region. The molecules with initial relative velocity η_B will arrive at velocity $-\eta_B$, after half an orbit around the phase space.

$$\frac{d^2x}{dt^2} = -a(t)\sin[q(x-v_Lt)], \qquad (5)$$

where $a(t) = \alpha q E_1(t)E_2(t)/(2m)$ is the maximum force per unit mass, m is the molecular mass.

For the convenience of studying the dynamics in the traveling optical lattice we introduce the reference frame,

$$\theta = q(x-v_Lt), \qquad (6)$$

moving with the optical lattice, and a normalized time

$$\tau = t\omega_0, \qquad (7)$$

where $\omega_0 = \sqrt{qa}$ is the harmonic resonant frequency in the optical lattice. Since we are interested in the motion of molecules within a pulse of constant intensity a is now time independent. In the traveling reference frame, the optical lattice is a standing wave, and we define a normalized velocity η by

$$\eta = \frac{d\theta(\tau)}{d\tau}. \qquad (8)$$

The normalized velocity η is related to the velocity v in the laboratory frame by

$$\eta = (v-v_L)/v_n, \qquad (9)$$

where $v_n = \omega_0/q$. From Eq. (5), we arrive at the normalized equation of motion,

$$\frac{d\eta}{d\tau} + \sin(\theta) = 0, \qquad (10)$$

which is the well-known equation of motion of a nonlinear pendulum [43–45]. The dynamics of Eq. (10) has been studied previously for nonlinear pendulums [43–46], and we briefly review the dynamics in the phase space (θ,η) as shown in Fig. 2, where each line is an equal-energy line. The

dotted lines are separatrix, which define the enclosed region where molecules are trapped. Outside this region molecules are not trapped by the lattice potential. The arrows in the figure show the direction of motion of molecules within the phase space. Molecules in the untrapped region move from one potential well to the other keeping their initial motion direction unchanged, while those in the trapped region move along closed trajectories. In the following two sections, using the phase-space plot in Fig. 2, we will explore the mechanisms for decelerating molecules to zero velocity, and bunching of molecules with the traveling optical lattice.

A. Creating nearly stationary molecules using reflection in the lattice frame

The dynamical process of reflection [41] in a lattice, as shown in Fig. 2, can be used to decelerate molecules to zero velocity. The upper thick solid line in the figure, corresponding to a beam velocity $\eta = \eta_B$, where the normalized beam velocity η_B is defined by

$$\eta_B \equiv (v_B - v_L)/v_n, \qquad (11)$$

shows an ensemble of molecules which have a narrow velocity distribution as produced by a cold supersonic beam. The lower thick solid line ($\eta = -\eta_B$) corresponds to the ensemble of molecules whose initial velocity $\eta = \eta_B$ has been reversed via motion along the closed trajectories shown in the figure. Three dynamical processes contributing to reflection of molecules are identified. The first involves molecules whose initial phases are between 0 and π and correspond to trajectories from point A to B in the figure. Here, the time required for reflection is shorter than half an oscillation period around the phase space. The second process involves molecules whose initial phases are symmetrical with $\theta=0$. In the diagram this corresponds to the molecules moving from F and C and to D and E, respectively. These molecules reverse their initial velocity after traveling half their orbit. A third process involves molecules whose initial phases are between $-\pi$ and 0, which are reflected after traveling more than a half of an orbit. These are molecules that travel from G to H in Fig. 2. When the lattice velocity is set to half the initial velocity of a molecular beam, v_B ($v_L = v_B/2$), the molecules reflected by the three processes now have zero velocity in the laboratory frame. Therefore, an ensemble of cold stationary molecules can be produced by turning off the optical fields at the time that the ensemble has been reflected.

If the lattice velocity is not equal to the half beam velocity ($v_L \neq v_B/2$), an ensemble of nearly stationary molecules can be obtained by switching off the optical fields when the ensemble is slowed to a normalized velocity $\eta_s \equiv -v_L/v_n$. As the value of η_s is not equal to $-\eta_B$, until $v_L = v_B/2$, the lines $\eta = \eta_B$ and $\eta = \eta_s$ in the phase space (θ, η) are not symmetric around the axis $\eta=0$, such that for cases where $v_L \neq v_B/2$, the reflection processes discussed above cannot be exploited. This is true especially for the second process which does not lead to the creation of stationary molecules. Without the second process, we will slow less molecules to zero velocity and thus the lattice velocity $v_L = v_B/2$ is opti-

mal for slowing molecules to a standstill. This conclusion is supported by the simulations of molecular deceleration as detailed in Sec. IV.

B. Bunching of molecules in the optical lattice resulting from conservation of phase space density

The trajectories in phase space as shown in Fig. 2 are plotted under the assumption that collision between molecules can be neglected when the pulse duration is shorter than the characteristic collision time of molecules in the molecular beam. Due to the collisionless environment, and the conservative motion of the molecules in the lattice, the phase-space density for the ensemble is unchanged with time [49]. Previously, the conservative feature of the phase-space density has been explored in bunching (squeezing or focusing) of particles. δ-kicked squeezing of atoms within optical lattices was investigated for atom lithography [35], while bunching of neutral atoms and neutrons with time-varying magnetic fields has been discussed [50–52] for the purpose of cooling. Most recently, longitudinal focusing of neutral polar molecules with time-varying electric fields was demonstrated for application to the storage of cold molecules and molecular optics [34].

Now we consider bunching of molecules within optical lattices and illustrate this process again using Fig. 2. The line $\eta = \eta_B$ shown in Fig. 2 can be considered to be molecules that are initially spread uniformly in position space and have a very narrow velocity width as is produced by a cold molecular beam. Molecules start to travel along their equal-energy lines in the phase space and therefore the width of distribution of the trapped molecules will increase in velocity space, while narrowing the distribution in position. When the velocity width of the distribution is at a maximum, spatial bunching is obtained. The position where the spatial bunching occurs depends on the lattice velocity. For example, for a molecular beam (horizontal dot-dashed line) with velocity $\eta_B = 0$ ($v_L = v_B$), molecules accumulate around $\theta = 0$ (vertical dot-dashed line) while the velocities of the trapped molecules spread from $\eta = -2$ to $\eta = 2$, after traveling one quarter of their orbits. If the relative velocity $\eta_B \neq 0$, or the lattice velocity $v_L \neq v_B$, the spatial bunching position will be changed from $\theta = 0$, because in this case the time for molecules to travel from the initial positions to $\theta = 0$ is dependent on initial positions. Therefore, we can alter the position of the spatial bunching within a potential well by choosing a different beam velocity, and similarly, we can manipulate the bunching in velocity space. The creation of stationary molecules using reflection of molecules in the lattice frame, discussed in Sec. II A, is one special case of bunching of molecules in velocity space. Thus, we can create an ensemble of nearly stationary molecules and simultaneously bunch the ensemble in velocity space.

III. KINETIC DESCRIPTION OF MOLECULAR MOTION IN THE OPTICAL LATTICE

In this section, we present a statistical description of the ensemble of molecules within the lattice in order to predict the distribution function of the molecular beam perturbed by

the lattice, as well as the efficiency of the deceleration and bunching processes. We consider a pulsed molecular beam with an initial temperature T and beam velocity v_B perturbed by the optical lattice. Initially, the ensemble of molecules is uniformly distributed in position space, and has a longitudinal velocity distribution function given by $f_0(v) = \exp[(v - v_B)^2/v_a^2]/(\sqrt{\pi} v_a)$, where $v_a = \sqrt{2K_B T/m}$ is the most probable velocity. After the optical fields are turned on, the evolution of the distribution function of the molecules within the one-dimensional traveling optical lattice can be described by the collisionless Boltzmann equation [47] when the duration of optical lattice is much shorter than the mean collision time. As the dipole force has little effect on transverse motion of molecules, the transverse distribution in the collisionless environment can be decoupled from longitudinal distribution [46]. We can therefore calculate the evolution of the longitudinal velocity and position distribution function of the gas using the one-dimensional collisionless Boltzmann equation,

$$\frac{\partial f(x,v,t)}{\partial t} + v\frac{\partial f(x,v,t)}{\partial x} + \frac{F_{\parallel}(x,t)}{m}\frac{\partial f(x,v,t)}{\partial v} = 0, \quad (12)$$

where $f(x,v,t)$ is the position and velocity distribution function, which satisfies the initial condition $f(x,v,t) = f_0(v)$. The dipole force $F_{\parallel}(x,t)$ exerted on a molecule is given by Eq. (4). Previously, the collective behavior of free molecular beams in dipole force experiments using short pulsed lasers have been well described by the one-dimensional collisionless Boltzmann equation [33,48].

The collisionless Boltzmann equation with an external periodic traveling force has been treated analytically for arbitrary initial conditions [46]. In the following analysis we briefly present the process for obtaining the analytical solution to Eq. (12).

To discuss how the distribution evolves within the phase space as a function of time, we apply the normalization transform given by Eqs. (6)–(8) and define the normalized distribution function by

$$f(\theta, \eta, \tau) = q f(x,v,t)/v_n. \quad (13)$$

Inserting Eqs. (6)–(8) and (13) into Eq. (12), the normalized distribution function $f(\theta, \eta, \tau)$ satisfies the normalized collisionless Boltzmann equation,

$$\frac{\partial f(\theta, \eta, \tau)}{\partial \tau} + \eta \frac{\partial f(\theta, \eta, \tau)}{\partial \theta} - \sin(\theta)\frac{f(\theta, \eta, \tau)}{\partial \eta} = 0. \quad (14)$$

From Eq. (14), the differentiation of $f(\theta, \eta, \tau)$ with respect to τ satisfies

$$\frac{df(\theta(\tau), \eta(\tau), \tau)}{d\tau} = 0, \quad (15)$$

and $\theta(\tau)$ and $\eta(\tau)$ satisfy Eqs. (8) and (10).

The function $f(\theta(\tau), \eta(\tau), \tau)$ can be interpreted as the probability density of a single molecule, and Eq. (15) shows that this probability density is conserved, i.e.,

$$f(\theta,\eta,\tau)=f(\theta,\eta,0)=\eta_m\exp[-\eta_m^{-2}(\eta(0)-\eta_D)^{-2}]/\sqrt{\pi},$$
$$(16)$$

where $\eta_m=v_a/v_n$ is the normalized most probable velocity.

In Eq. (16), the initial velocity of a molecule, $\eta(0)$, can be obtained by solving Eqs. (8) and (10). The velocity $\eta(0)$ is given by [46]

$$\eta(0)=\frac{\eta\,\mathrm{cn}(\tau,N)+\sin(\theta)\,\mathrm{sn}(\tau,N)\,\mathrm{dn}(\tau,N)}{1-\left[\sin\left(\dfrac{\theta}{2}\right)\mathrm{sn}(\tau,N)\right]^2}$$

$$(N\leqslant 1 \quad \text{for trapped molecules}) \qquad (17)$$

or

$$\eta(0)=\frac{\eta\,\mathrm{dn}\left(N\tau,\dfrac{1}{N}\right)+\sin(\theta)\,\mathrm{sn}\left(N\tau,\dfrac{1}{N}\right)\mathrm{cn}\left(N\tau,\dfrac{1}{N}\right)/N}{\left[\mathrm{cn}\left(N\tau,\dfrac{1}{N}\right)\right]^2+\left[\dfrac{\eta\,\mathrm{sn}\left(N\tau,\dfrac{1}{N}\right)}{2N}\right]^2}$$

$$(N>1 \quad \text{for untrapped molecules}), \qquad (18)$$

where

$$N=\sqrt{\eta^2/4+\sin(\theta/2)^2} \qquad (19)$$

and $\mathrm{cn}(\tau,N)$, $\mathrm{sn}(\tau,N)$, and $\mathrm{dn}(\tau,N)$ are, respectively, the Jacobian elliptical cosine, sine, and tangent functions [53,54].

IV. SLOWING AND VELOCITY BUNCHING OF AN ENSEMBLE OF MOLECULES

By using the analytical results presented in Sec. III, we investigate the deceleration and bunching of molecules in a traveling optical lattice. Here, we consider a translationally cold (1 K) carbon monoxide (CO) molecular beam with a velocity of $v_B=230$ m/s, which can be produced by a supersonic expansion [24]. The traveling optical lattice is produced by two counterpropagating optical plane waves. The lattice spatial frequency is chosen to be $q=1.57\times10^7$/m, and the optical lattice velocity v_L is set to the optimal value of $v_L=v_B/2=115$ m/s. The optical fields are chosen to have amplitudes $E_1=E_2=2.5\times10^9$ V/m corresponding to an intensity $I=8.29\times10^{11}$ W/cm^2, which is much lower than the dissociative ionization threshold intensity for CO molecules [55]. This produces a potential well depth of 49 K which enables trapping of molecules traveling at 115 m/s relative to the lattice velocity. The lattice beams ($\lambda_1\approx\lambda_2=800$ nm with $\omega_1\approx\omega_2=2.36\times10^{15}$ rad/s) are detuned from the first single photon allowed electronic state [the R(0) line of $A\,^1\Pi-X\,^1\Sigma^+(0,0)$ transition at $\lambda=154.4$ nm] [56] by 9.8×10^{15} rad/s. This value is approximately three orders of magnitude greater than the Rabi frequency (1.0×10^{13} rad/s) calculated for this transition using E_1 and E_2 given above [57].
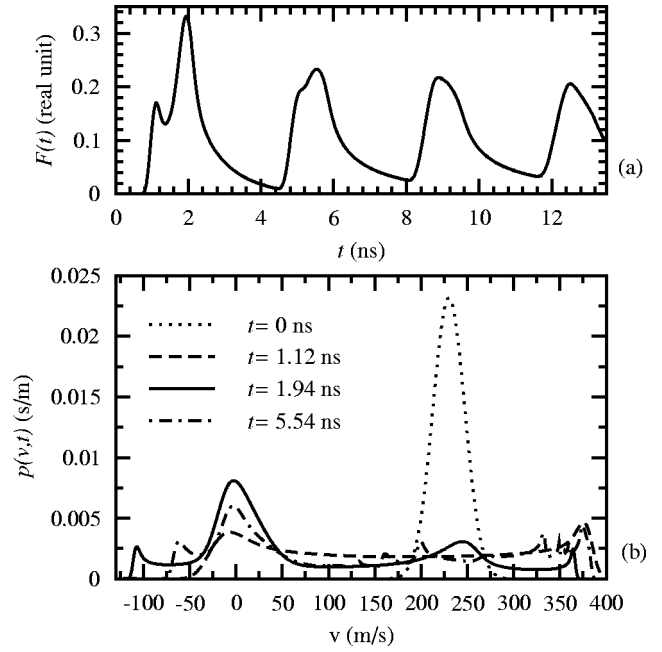
In our scheme, a fraction of stationary molecules can be

FIG. 3. (a) A plot of the fraction of molecules with velocity between -25 m/s and 25 m/s as a function of pulse duration. The CO molecular beam has an initial velocity 230 m/s and a temperature of 1 K which is perturbed by an optical lattice with a velocity 115 m/s. (b) The initial distribution function (dotted), and the distribution functions for three pulse durations, after the lattice is turned on. The three pulse durations correspond to the first three peaks in Fig. 3(a).

created by switching off the optical fields when the molecules are reflected in the lattice frame. Therefore, the pulse duration is critical for implementation of our scheme when a significant fraction of stationary molecules is required. In the study of the reflection of neutral molecules and atoms by a pulsed optical lattice [40,41,59], the pulse duration is set to be a half period of the motion around the phase space by assuming simple harmonic motion. However, as a number of molecules do not undergo harmonic motion, the pulse duration determined by their approach cannot be optimal [46]. In this paper, we determine the optimal pulse duration by maximizing the slowed fraction of molecules, $F(t)$, in the velocity range of 1 K (~25 m/s for CO molecule) [60], calculated by $F(t)=\int_{(-25-v_B)/v_n}^{(25-v_B)/v_n}\int_{-\pi}^{\pi}f(\theta,\eta,\tau)d\theta d\eta/(2\pi)$, where $f(\theta,\eta,\tau)$ is calculated with Eq. (17) or (18) depending on the corresponding parameter N defined by Eq. (19), and τ is related to t through Eq. (7). Figure 3(a) shows the calculated fraction $F(t)$ as a function of pulse durations t_d. As the molecules travel around the phase space of Fig. 2 the fraction centered at zero velocity is almost periodic and slowly decreases after each orbit around the phase space. The first three maxima occur at $t_d=1.12$ ns, 1.94 ns, and 5.54 ns. The first peak which occurs at $t_d=1.12$ ns takes less than half of the period expected from simple harmonic motion. This peak is produced by the first reflection process (A to B) in Fig. 2. In contrast, the largest slowed fraction which occurs at $t_d=1.94$ ns takes longer than half the period of simple harmonic motion and corresponds to the three pro-

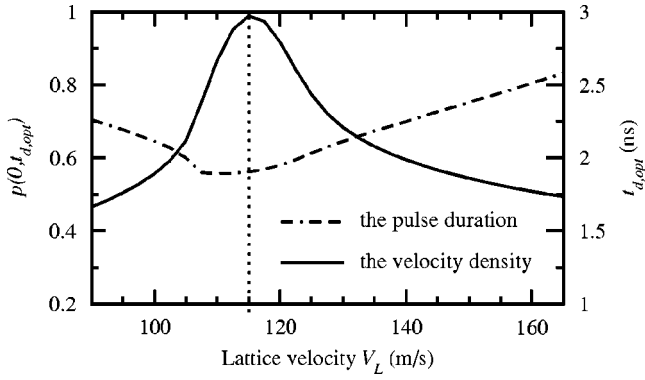FIG. 4. A graph of the optimal pulse duration $t_{d,opt}$ (dot-dashed line) and the velocity distribution at zero velocity, $p(0,t_{d,opt})$ (solid line), as a function of the lattice velocity v_L. The velocity distribution function $p(0,t_{d,opt})$ has a bell shape with the summit at the optimal lattice velocity 115 m/s, denoted by a dotted line. The rate of decrease of the velocity distribution function $p(0,t_{d,opt})$ with respect to the lattice velocity at the right side of the dotted line is smaller than that at the left side because the motion of molecules is more closely approximated by simple harmonic motion as the lattice velocity increases.

FIG. 5. A plot showing the sensitivity of optimal velocity density at zero velocity, $p(0,t_{opt})$, and pulse duration, t_{opt}, as a function of intensity. As the intensity increases the potential-well depth increases, and the normalized beam velocity decreases via Eq. (11). Thus, more molecules are trapped and reflected, and the half period decreases. The optimal pulse duration t_{opt} decreases when the optical intensity increases, and the corresponding velocity density $p(0,t_{opt})$ increases. This figure demonstrates that a small change in the intensity does not significantly change the optimal velocity density and pulse duration.

cesses (A to B, C to E, and F to D and G to H) in Fig. 2. This corresponds to a maximum slowed fraction of 33.4% of the total number of molecules. The following peaks occur because of the periodic nature of molecular motion in the potential wells. As the molecules that contribute to the second peak have different periods, at a later time not all of them arrive at the same velocity $v=0$ at the same time. Consequently, the peak height decreases with time as shown in Fig. 3(a). In Fig. 3(b), we plot the velocity distribution function $p(v,t)$, given by $p(v,t)=\int_{-\pi}^{\pi}f(\theta,(v-v_L)/v_n,t)d\theta/(2\pi v_n)$, for the first three peaks. This figure shows that by choosing a suitable pulse duration we can create a fraction of nearly stationary molecules which has an approximately Gaussian distribution centered at zero velocity, indicating a bunching in velocity space. Our mechanism for creating stationary molecules is to use reflection of molecules in the lattice frame. However, the velocity distribution shown in Fig. 3(b) does not resemble the initial distribution, because of anharmonicity of molecular motion in the lattice. Therefore, it is essential to use the kinetic description presented in Sec. III to determine the optimal pulse duration, rather than the assumption of simple harmonic motion [40,41,46].

To understand how different lattice velocities affect deceleration in the lattice, we plot in Fig. 4 the optimal time t_{opt} (dot-dashed line) for producing the maximum fraction of slowed molecules as a function of lattice velocity. Also in this figure, we plot the peak height, of the velocity distribution function at zero velocity at the optimum time, $p(0,t_{opt})$, as a function of lattice velocity. The graph of the peak value of the velocity distribution function $p(0,t_{opt})$ has an asymmetric bell shape with a maximum occurring when the lattice velocity is half the beam velocity. The maximum indicates that this velocity is optimal for creating the maximum fraction of stationary molecules. When the lattice velocity is
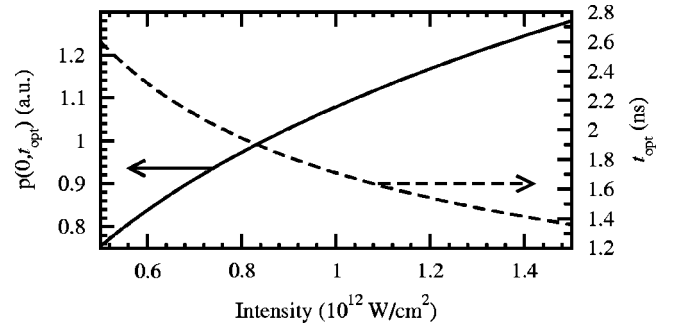
greater than this optimum velocity the motion of a larger fraction of the trapped molecules is more closely described by simple harmonic motion. Therefore, the number of slowed molecules at lattice velocities higher than the optimum value decreases more slowly when compared to lattice velocities lower than the optimum. For a lattice velocity that deviates by ± 5 m/s from half the beam velocity (optimum velocity), the optimal pulse duration t_{opt}, and the velocity distribution at zero velocity, $p(0,t_{opt})$, only decrease by 5% and 8%, respectively, from their optimum values, indicating little sensitivity to small variations in lattice velocity. This implies that in an experiment that the frequency difference of the pulsed laser beams must be controlled within ≈ 10 MHz. The type of frequency stability can be attained using nanosecond pulsed lasers that are injection seeded with a narrow linewidth (<10 KHz) continuous wave (CW) laser (Model 126 Lightwave Electronics for a Nd:YAG laser system) or by pulsed amplified systems.

We also have investigated how the intensity of the optical fields affects the velocity density at zero velocity, $p(0,t_{opt})$, as well as the optimal pulse duration t_{opt}. In Fig. 5, the beam velocity of the CO molecular beam is the same as that used in Fig. 3 where the lattice velocity is half the molecular-beam velocity. As the intensity increases the potential-well depth increases, and the normalized beam velocity decreases via Eq. (11). Thus, more molecules are trapped and reflected, and the half period within the potential decreases. This is why in the figure the optimal pulse duration t_{opt} decreases when the optical intensity increases, and the corresponding velocity density $p(0,t_{opt})$ increases. In an experiment a smooth temporal profile that varies by approximately less than 5% can be obtained by a pulsed amplified CW system that is electro-optically sliced to produce a flat top temporal profile. If the intensity increases by 5%, no particles are lost from the potential. However, when the intensity drops by 5% Fig. 5 indicates that the velocity density would decrease in the same proportion.
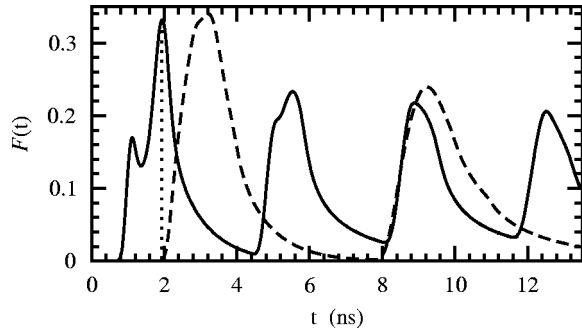
FIG. 6. The fraction of nearly stationary CO molecules (solid line) and Xe atoms (dashed line) as a function of pulse duration. Due to the large difference in polarizability to mass ratio, CO molecules can be slowed down to nearly zero velocity at an earlier time than Xe atoms. Therefore, by choosing a suitable pulse duration, only the CO molecules and not the Xe buffer gas are slowed down to zero velocity.

Simultaneous separation of the slowed molecules from the buffer gas

The slow cold molecules produced by our method could be used for further cooling and other applications. However, beams of light molecules are normally mixed with a high-density buffer gas such as Xe in a supersonic expansion. For many applications, the buffer gas would need to be removed from the ensemble of slow cold molecules. Recently, we have shown that different species with different polarizability

to mass ratio can be separated in velocity space [58]. There-fore, we compare the fraction of the nearly stationary CO molecules with that of the nearly stationary heavy Xe, as shown in Fig. 6. In this figure, the temporal evolution of the slowed fraction of CO molecules (solid line) and Xe molecules (dashed line) shows that the stationary CO molecules are produced earlier than the stationary Xe atoms. This is because the polarizability to mass ratio for Xe is less than half that for CO, and the maximum force per unit mass for Xe is lower than that for CO. For a pulse duration $t = 1.94$ ns, the number of the nearly stationary Xe atoms is about 0.6% of the total Xe atoms. If we assume that 95% Xe atoms are seeded in the gas mixture to create a CO beam with 230 m/s [24], at $t = 1.94$ ns, the number of Xe atoms presented in the stationary gas mixture is about 25.7%. For a pulse duration of $t = 1.83$ ns, the percentage of Xe molecules in the nearly stationary gas mixture is about 0.22%, while a high fraction ($\sim 30.1\%$) of stationary CO molecules is maintained. In conclusion, taking advantage of the large difference of the polarizability to mass ratio between the gas molecules and the buffer Xe atoms, we can obtain a high fraction of nearly stationary molecules mixed with a low fraction of buffer gas by choosing a suitable pulse duration.

V. SPATIAL BUNCHING OF AN ENSEMBLE OF MOLECULES

Figures 7(a) and 7(b) are contour plots of the velocity distribution $p(v,t)$ and the number density (spatial distribu-
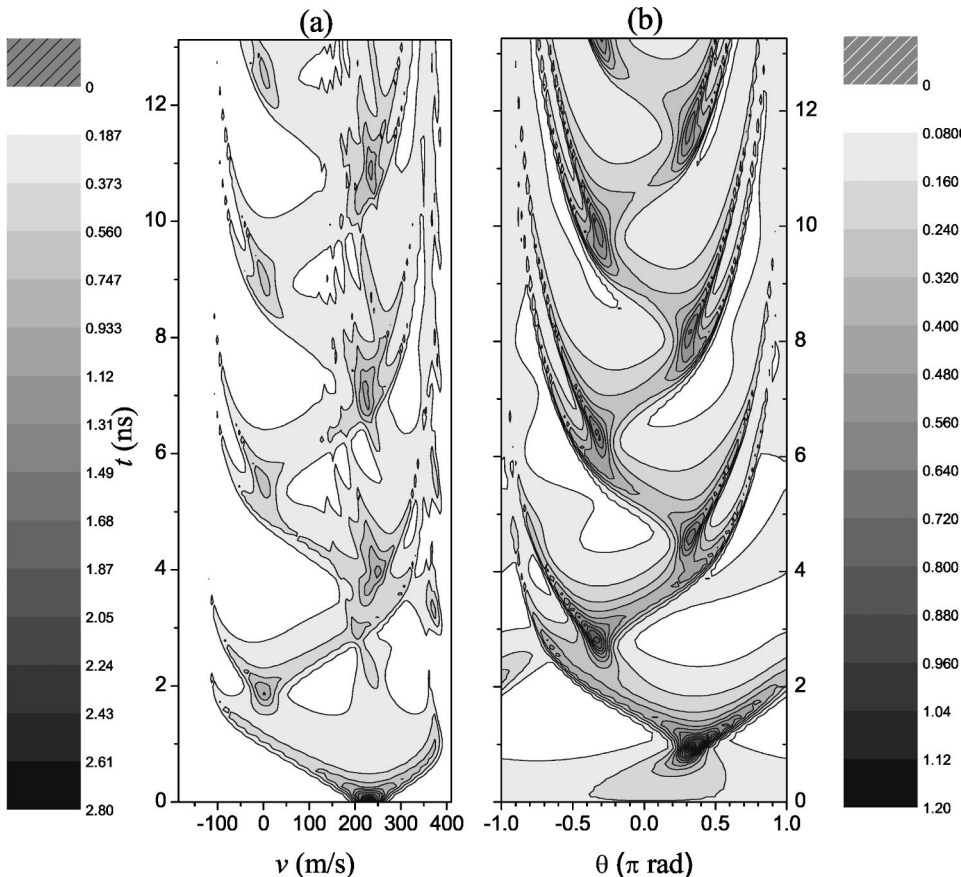

FIG. 7. Contour plots of the velocity distribution function [Fig. 7(a)], and the number density [Fig. 7(b)], for the molecules in the optical lattice with velocity 115 m/s. The intensity of the lattice fields and the spatial frequency of the lattice, as well as the initial temperature and beam velocity of the molecular jet, are the same as used in Fig. 3. Initially, the ensemble of molecules has a narrow velocity distribution and is spread uniformly in the lattice. After the optical fields are turned on, the increase in the width of velocity distribution is accompanied by the bunching of the molecules in the lattice, because of the conservation of the phase-space density. Therefore, by choosing a suitable pulse duration, we can realize bunching in position or velocity space.
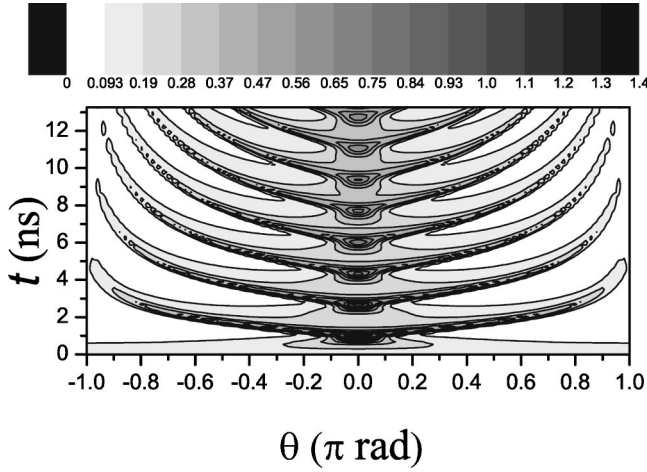
FIG. 8. Contour plot of the number density of molecules in an optical lattice with velocity 230 m/s. The initial velocity and temperature of the molecular beam, and the optical intensity as well as the spatial frequency of the lattice are the same as those used in Fig. 7. In this scheme, the lattice velocity is set equal to the beam velocity. Note that the molecules which initially have a uniform distribution in space, can be focused at the phase $\theta=0$, after the optical fields are turned on. Compared with Fig. 7, we show that the bunching position can be altered by using the lattice velocity.
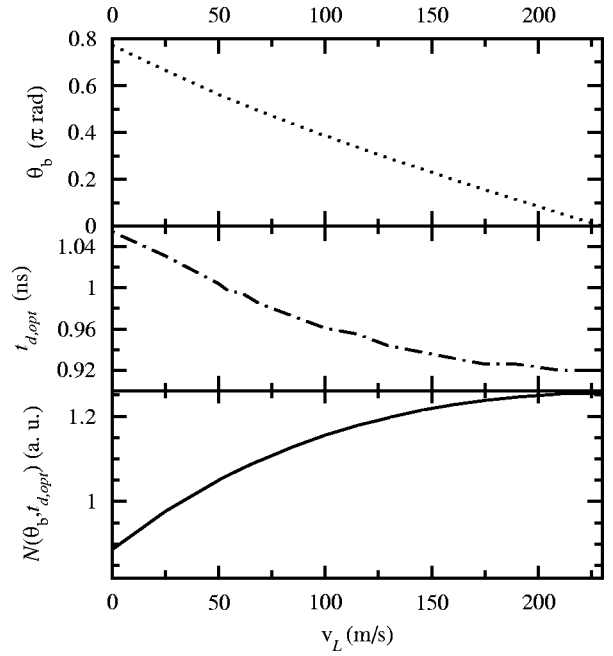

FIG. 9. Graphs of bunching position θ_b (dotted line), the highest number of density $N(\theta_b, t_{d,opt})$ (solid line) and, corresponding optimal pulse duration $t_{d,opt}$ (dot-dashed line) as a function of the lattice velocity v_L.

tion) $N(\theta,t)=\int_{-\infty}^{\infty}f(\theta,\eta,\tau)d\eta$, respectively, for the CO molecular beam which is discussed in Sec. IV. Initially, the ensemble of molecules are uniformly distributed in position space, but narrowly distributed in velocity space. After the optical fields are turned on, the spatial distribution begins to narrow, while the velocity distribution expands due to the conservation of phase-space density. These figures show that spatial bunching and velocity bunching can be obtained at different times. Velocity bunching was discussed in Sec. IV, and in this section we consider the spatial bunching. The spatial bunching appears first at $\theta=0.34\pi$, and then at $\theta=-0.34\pi$. Due to the periodic anharmonic motion, the bunching reoccurs almost periodically, and the first bunch is the narrowest.

To see how the traveling lattice velocity affects the spatial bunching, we show a contour plot of the number of CO molecules in the optical lattice in Fig. 8 when the lattice velocity is equal to the beam velocity. The other parameters used in this plot are the same as those in Fig. 7. Compared to Fig. 7(b), the spatial bunching position in Fig. 8 is shifted to $\theta=0$ and the number density is increased. In Fig. 9, we further study a bunching position θ_b and the highest number density $N(\theta_b, t_{opt})$ as well as the optimal pulse duration t_{opt} as a function of the lattice velocity. This figure shows that the bunching position can be adjusted by the traveling lattice, and the highest number density is an increasing function of the lattice velocity while corresponding optimal pulse duration decreases, because the anharmonicity decreases as the lattice velocity increases. However, when the lattice velocity increases to 205 m/s, the highest number density saturates because the contribution to the spatial bunching is dominated by simple harmonic motion.

VI. DECELERATION USING GAUSSIAN PULSES IN A SUPERSONIC BEAM

In Secs. II and III, we have investigated the bunching of slow cold molecules in a molecular beam with a far-off-resonant traveling optical lattice using a flat top temporal intensity profile. Although this pulse shape may be realized with electro-optic chopping techniques, it is instructive to study how our scheme would perform using the more common Gaussian shaped temporal profile. We now consider a lattice produced by two Gaussian pulses whose electric field profiles are described by $E(t)=E_0\exp[-t^2/(2t_\sigma^2)]$, where E_0 is the maximum amplitude of the electric fields, and t_σ is e^{-1} width of the pulse intensity.

The velocity distribution of CO molecules produced by Gaussian pulses with $t_\sigma=1.12$ ns is shown in Fig. 10. This velocity distribution is calculated by numerical solution of the Boltzmann equation [41]. As before the molecules have an initial velocity of 230 m/s at 1 K, and the peak electric field is $E_0=2.5\times10^9$ V/m. The major features of the velocity distribution function produced by the top hat and Gaussian temporal profiles are similar indicating that both can be used to create slow cold molecules with comparable efficiency. For 5% CO contained within Xe buffer gas at 2 atm backing pressure we estimate the number density of CO in a pulsed supersonic beam to be 1×10^{12} cm^{-3}. For a Gaussian pulse with a transverse width of 100 μm, and a half Rayleigh range of 3.5 mm, the number of molecules in the lattice can be as high as 1×10^8. The nearly stationary molecules produced with our method is predicted to be about 33%, therefore up to 3×10^7 molecules could be confined in a trap with 1 K depth for CO molecules. This is a conservative value which will depend on the experimental geometry. The
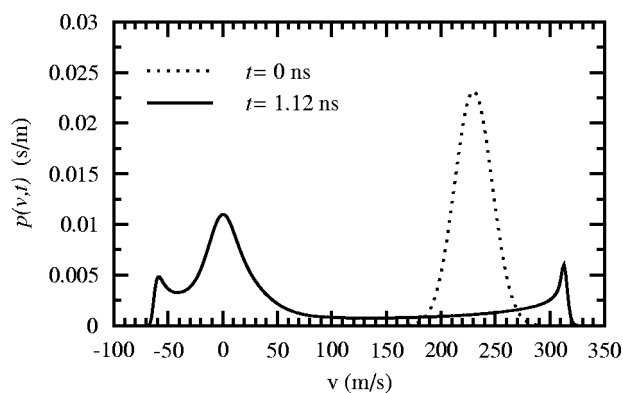
FIG. 10. The velocity distribution of molecules produced by an optical lattice formed by two counterpropagating fields with a Gaussian temporal intensity profile. The peak intensity of the Gaussian pulses is 8.29×10^{11} W/cm^2, and the e^{-1} pulse width is 1.2 ns. The lattice velocity and the beam velocity, as well as the initial temperature, are the same as those used in Fig. 3. For comparison, the initial velocity distribution function is plotted and shown as a dotted line.

time for experimentation is limited by the available vacuum in the deceleration region as the collision frequency (100 Hz) of the slowed with the unslowed molecules is not significant on the time scale of jet pulse (80 μs). Therefore, due to the low density in the jet there are essentially no interactions between the slowed and unslowed molecules. This has been demonstrated in experiments that have slowed jet cooled polar molecules using electrostatic techniques [26,27].

VII. SUMMARY AND REMARKS

We have analyzed the capability of using a traveling optical lattice to decelerate trapped molecules in a pulsed free molecular jet, and have found that the optimal lattice velocity for obtaining the highest fraction of nearly stationary molecules is half of the jet velocity. The mechanism for creating stationary molecules is the reflection in the traveling lattice frame whereby the reflected molecules have zero velocity in the laboratory frame. We have also shown that the molecules can be bunched in velocity space or position space, while keeping the initial phase-space density unchanged. An analytical expression for the velocity and position distribution function of the molecular beam is given by using a general analytical solution to the collisionless Boltzmann equation with an external periodic traveling force [46].

With our analytical solution, we can determine the fraction of molecules decelerated by the traveling potential well, and calculate the number density in order to predict the efficiency of the deceleration and bunching processes. We have shown that a significant fraction ($\sim 33\%$) of CO molecules in a molecular beam, with velocity 230 m/s and translational temperature of 1 K, can be decelerated to zero velocity and simultaneously bunched in velocity space. When there is a large difference of polarizability to mass ratio between the buffer gas and the CO molecules in the pulsed jet, the buffer gas can be precluded from the fraction of stationary molecules by choosing a suitable pulse duration. Further, we show that the traveling optical lattice can be used to longitudinally focus (bunch) an ensemble of molecules in position space, and the focus position can be adjusted by optical lattice velocity. The control of molecular distribution in space may benefit nanoscale molecular deposition [35,36].

Our approach is in some respects similar to a Stark deceleration or time-varying electric fields which can be applied to polar molecules [24–29]. Both use the trapped dynamics of a molecule in potential well, but in our approach, the Stark energy averaged over an optical period is zero, and the induced dipole plays a role in manipulating the velocity distribution of molecular beams. In the Stark deceleration schemes, the velocity of the traveling potential well is lowered gradually for decelerating molecules and many stages are needed, in contrast, our method uses a single optical lattice at constant velocity. In the electrostatic method, the deceleration of the molecular beam, and the velocity bunching of cold molecules, must be performed in two successive steps. However, in our method, deceleration and bunching can be completed simultaneously with a single optical pulse.

The optical microlinear decelerator [33] and our scheme can be used for the manipulation of all molecular beams, since we use the second-order Stark effect. The former method has the advantage that lower intensity optical fields ($\sim 10^{10}$ W/cm^2), chirped over durations of 100's of nanoseconds, can be used to decelerate molecular beams. In this case both the buffer gas and the molecular species are decelerated simultaneously in the lattice which may be undesirable in some applications of cold molecules. Our scheme which uses fixed frequency, shorter pulses in the nanosecond regime, uses higher intensity fields ($\sim 10^{12}$ W/cm^2) to create cold stationary molecules and is capable of both bunching in velocity and phase. Additionally, it can separate the buffer gas from the slowed cold molecules of interest.

[1] G. Meijer, Chem. Phys. Chem. **3**, 495 (2002).
[2] F. Masnou-Seeuws and P. Pillet, Adv. At., Mol., Opt. Phys. **47**, 53 (2001).
[3] E. Bodo, F.A. Gianturco, and A. Dalgarno, J. Chem. Phys. **116**, 9222 (2002).
[4] N. Balakrishnan, and A. Dalgarno, Chem. Phys. Lett. **341**, 652 (2001).
[5] R. Krems and A. Dalgarno, J. Chem. Phys. **117**, 118 (2002).
[6] J.L. Bohn, Phys. Rev. A **63**, 052714 (2001).

[7] N. Balakrishnan, A. Dalgarno, and R.C. Forrey, J. Chem. Phys. **113**, 621 (2000).
[8] K. Burnett, P.S. Julienne, P.D. Lett, E. Tiesinga, and C.J. Williams, Nature (London) **416**, 225 (2002).
[9] P. Zoller, Nature (London) **417**, 493 (2002).
[10] E.A. Donley, N.R. Claussen, S.T. Thompson, and C.E. Wieman, Nature (London) **417**, 529 (2002).
[11] J.T. Bahns, W.C. Stwalley, and P.L. Gould, J. Chem. Phys. **104**, 9689 (1996).

[12] P.D. Lett, P.S. Julienne, and W.D. Phillips, Annu. Rev. Phys. Chem. **46**, 423 (1995).

[13] P.D. Lett, K. Helmerson, W.D. Phillips, L.P. Ratliff, S.L. Rolston, and M.E. Wagshul, Phys. Rev. Lett. **71**, 2200 (1993).

[14] G. Zinner, T. Binnewies, F. Riehle, and E. Tiemann, Phys. Rev. Lett. **85**, 2292 (2000).

[15] A. Fioretti, D. Comparat, A. Crubellier, O. Dulieu, F. Masnou-Seeuws, and P. Pillet, Phys. Rev. Lett. **80**, 4402 (1998).

[16] J.D. Miller, R.A. Cline, and D.J. Heinzen, Phys. Rev. Lett. **71**, 2204 (1993).

[17] C. Gabbanini, A. Fioretti, A. Lucchesini, S. Gozzini, and M. Mazzoni, Phys. Rev. Lett. **84**, 2814 (2000).

[18] J.P. Shaffer, W. Chalupczak, and N.P. Bigelow, Phys. Rev. Lett. **82**, 1124 (1999).

[19] U. Schlöder, C. Silber, and C. Zimmermann, Appl. Phys. B: Lasers Opt. **73**, 801 (2001).

[20] A.N. Nikolov, J.R. Ensher, E.E. Eyler, H. Wang, W.C. Stwalley, and P.L. Gould, Phys. Rev. Lett. **84**, 246 (2000).

[21] B. Laburthe Tolra, C. Drag, and Pierre Pillet, Phys. Rev. A **64**, 061401 (2001), and references therein.

[22] J.D. Weinstein, R. deCarvalho, T. Guillet, B. Friedrich, and J.M. Doyle, Nature (London) **395**, 148 (1998).

[23] D.R. Miller, in *Atomic and Molecular Beam Methods*, edited by G. Scoles (Oxford University Press, New York, 1988), Vol. 1.

[24] H.L. Bethlem, G. Berden, and G. Meijer, Phys. Rev. Lett. **83**, 1558 (1999).

[25] J.A. Maddi, T.P. Dinneen, and H. Gould, Phys. Rev. A **60**, 3882 (1999).

[26] H.L. Bethlem, G. Berden, F.M.H. Crompvoets, R.T. Jongma, A.J.A. van Roij, and G. Meijer, Nature (London) **406**, 491 (2000).

[27] H.L. Bethlem, G. Berden, A.J.A. van Roij, F.M.H. Crompvoets, and G. Meijer, Phys. Rev. Lett. **84**, 5744 (2000).

[28] F.M.H. Crompvoets, H.L. Bethlem, R.T. Jongma, and G. Meijer, Nature (London) **411**, 174 (2001).

[29] H.L. Bethlem, F.M.H. Crompvoets, R.T. Jongma, S.Y.T. van de Meerakker, and G. Meijer, Phys. Rev. A **65**, 053416 (2002).

[30] M. Gupta and D. Herschbach, J. Phys. Chem. A **105**, 1626 (2001).

[31] M. Gupta and D. Herschbach, J. Phys. Chem. A **103**, 10 670 (1999).

[32] B. Friedrich, Phys. Rev. A **61**, 025403 (2000).

[33] P.F. Barker and M.N. Shneider, Phys. Rev. A **66**, 065402 (2002).

[34] F.M.H. Crompvoets, R.T. Jongma, H.L. Bethlem, A.J.A. van Roij, and G. Meijer, Phys. Rev. Lett. **89**, 093004 (2002).

[35] M. Leibscher and I.S. Averbukh, Phys. Rev. A **65**, 053816 (2002).

[36] B.K. Dey, M. Shapiro, and P. Brumer, Phys. Rev. Lett. **85**, 3125 (2002).

[37] T. Takekoshi and R.J. Knize, Opt. Lett. **21**, 77 (1996).

[38] C. Keller, J. Schmiedmayer, A. Zeilinger, T. Nonn, S. Purr, and G. Rempe, Appl. Phys. B: Lasers Opt. **69**, 303 (1999).

[39] H. Sakai, A. Tarasevitch, J. Danilov, H. Stapelfeldt, R.W. Yip, C. Ellert, E. Constant, and P.B. Corkum, Phys. Rev. A **57**, 2794 (1998). Here the prospect of applying well-advanced technologies of pulse shaping to manipulate molecular distribution in an optical lattice was discussed.

[40] P. Ryytty and M. Kaivola, Phys. Rev. Lett. **84**, 5074 (2000).

[41] P. Ryytty and M. Kaivola, Eur. Phys. J. D **12**, 415 (2000).

[42] Y.B. Ovchinnikov, J.H. Müller, M.R. Doery, E.J.D. Vredenbregt, K. Helmerson, S.L. Rolston, and W.D. Phillips, Phys. Rev. Lett. **83**, 284 (1999).

[43] R.Z. Sagdeev, D.A. Usikov, and G.M. Zaslavsky, *Nonlinear Physics: From the Pendulum to Turbulence and Chaos* (Harwood Academic Publishers, Chur, 1988).

[44] P. Hagedorn, *Nonlinear Oscillations* (Oxford University Press, Oxford, 1978).

[45] C. Hayashi, *Nonlinear Oscillations in Physical Systems* (McGraw-Hill, New York, 1964).

[46] Guangjiong Dong, Weiping Lu, and P.F. Barker, Phys. Rev. E **68**, 016607 (2003).

[47] K. Huang, *Statistical Mechanics* (Wiley, New York, 1987).

[48] J.H. Grinstead and P.F. Barker, Phys. Rev. Lett. **85**, 1222 (2000).

[49] C. Cercignani, *The Boltzmann Equation and its Applications* (Springer-Verlag, New York, 1988).

[50] S. Chu, J.E. Bjorkholm, A. Ashkin, J.P. Gordon, and L.W. Hollberg, Opt. Lett. **11**, 73 (1986).

[51] H. Ammann and N. Christensen, Phys. Rev. Lett. **78**, 2088 (1997).

[52] J. Summhammer, L. Niel, and H. Rauch, Z. Phys. B: Condens. Matter **62**, 269 (1986).

[53] M. Abramowitz and I.A. Stegun, *Handbook of Mathematical Functions with Formulas, Graphs, and Mathematical Tables* (National Bureau of Standards, Washington, D.C., 1964).

[54] S. Zhang and J. Jin, *Computation of Special Functions* (Wiley, New York, 1996).

[55] D. Normand, L.A. Lompre, and C. Cornaggia, J. Phys. B **25**, L497 (1992). They created alignment of a thermal ensemble of CO molecules with a strong pulsed laser field (intensity $\sim 10^{14}$ W/cm^2, pulse duration between 1 and 30 ps), prior to their dissociative ionization.

[56] A.C. Le Floch, F. Launay, J. Rostas, R.W. Field, C.M. Brown, and K. Yoshino, J. Mol. Spectrosc. **121**, 337 (1987).

[57] M. Eidelsberg and F. Rostas, J. Chem. Phys. **96**, 5585 (1996).

[58] Guangjiong Dong, Weiping Lu, and P.F. Barker, J. Chem. Phys. **118**, 1728 (2003).

[59] The manipulation of the velocity distribution of atoms with a pulsed traveling optical lattice has been mentioned by Ryytty *et al.*, in studying a pulsed standing wave mirror for neutral atoms [41], where the pulse duration is determined with the assumption of simple harmonic motion.

[60] Metastable CO molecules with velocities below 25 m/s can be trapped in an electric quadrupole trap [24].